Phys. Chem. Liq., 1994, Vol. 26, pp. 237–246
Reprints available directly from the publisher
Photocopying permitted by license only

NONEQUILIBRIUM MOLECULAR DYNAMICS OF A DENSE IONIC FLUID

I. M. SVISHCHEV and P. G. KUSALIK

Department of Chemsitry, Dalhousie University, Halifax, Nova Scotia, B3H 4J3, Canada

(Received January 20, 1993)

Although the structural and transport properties of molten salts have been frequently examined in equilibrium molecular dynamics (MD) simulations, relatively little is known about these systems in nonequilibrium conditions. In this article we report results from nonequilibrium molecular dynamics (NEMD) simulations of a dense ionic fluid composed of charged soft spheres and compare these with equilibrium MD simulation data for the same system. Using Gaussian isokinetic equations of motion, the response of the system to applied electrical fields, varying in magnitude and frequency, was investigated in detail. The frequency dependent electrical conductivity was evaluated in nonequilibrium conditions and was found to be in good quantitative agreement with the spectrum of current fluctuations in the equilibrium ensemble. In order to follow the distortion of the liquid structure in external electric fields we also considered the direction-dependent distributions of charges in an ionic flow.

KEY WORDS: Dense ionic fluid, nonequilibrium dynamics.

1 INTRODUCTION

Transport coefficients provide a basis for the description of fluid dynamics, and detailed information in this area now comes to a large extent from MD simulations. Recently, the more traditional approach of calculating transport coefficients from equilibrium time-correlation functions using Green-Kubo integrands has been superseded in many aspects by NEMD techniques which enable us to determine transport coefficients from the response of the system to applied fields[1,2]. For simple monatomic liquids NEMD has proven to be a more efficient approach for the study of transport phenomena associated with the collective response of these systems[1]. However, very few investigations of the transport processes in the systems with long-range interactions (such as molten salts and electrolyte solutions) have been carried out using NEMD and questions still remain concerning both accuracy and computational efficiency. We report results from NEMD simulations of a dense ionic fluid with state parameters corresponding to those of a typical molten salt. The same system has been the subject of a previous equilibrium study[10]. In this comparative study the complex frequency dependence of the spectrum of electrical conductivity of this

molten salt will be of particular interest. As in a physical experiment, the spectrum of conductivity will be recovered directly from the response of the system to applied electric fields. Both static and oscillating fields have been employed in these NEMD simulations.

A further aim of the study is to examine the changes in ionic packing in an nonequilibrium molten electrolyte subjected to a strong electric field. This has been a somewhat neglected area compared with the extensive literature that exists for equilibrium structural properties[9,10,12,13]. Since the present NEMD simulations closely mimic the behavior of the corresponding nonequilibrium systems, we have determined nonequilibrium binary ionic distributions in order to provide insights into the structure of ionic flows.

2 IONIC DYNAMICS IN EXTERNAL FIELDS

The new element in nonequilibrium simulation techniques is the utilization of more general non-Newtonian equations of motion[1]. With these equations of motion, which include a perturbation field as part of the statistical mechanical description, it is possible to generate the corresponding nonequilibrium steady states. Since the applied field usually does work on the system these equations of motion employ appropriate thermostatting mechanisms to remove dissipative heat allowing a steady state to be maintained during the simulation run. Several models of thermostatted dynamics have been proposed[1–4], and a number of computational algorithms have been developed for the evaluation of transport coefficients, principally in Lennard-Jones systems[3–8]. In our calculations of electrical conductivity and of the structure of nonequilibrium molten salt we used the Gaussian (isokinetic) NEMD algorithm of Evans and Morriss[1,4a]. This algorithm was utilized originally in "color current" computer experiments with Lennard-Jones particles and can be applied easily to ionic dynamics simulations.

The Gaussian isokinetic equations of motion that govern the behavior of spherical particles with charge, Q_i, and mass, m, in an external electric field, E_z, (applied in Z-direction) are[1,4a]

$$\dot{\mathbf{q}}_i = \frac{\mathbf{p}_i}{m} = \mathbf{v}_i \tag{1a}$$

and

$$\dot{\mathbf{p}}_i = \mathbf{F}_i + \mathbf{z}Q_iE_z - \alpha\left(\mathbf{p}_i - \mathbf{z}\,\frac{mQ_iJ_z}{Q_i^2N}\right). \tag{1b}$$

In Eqs. (1) $\mathbf{q}_i$ and $\mathbf{p}_i$ are, respectively, the position coordinates and momenta, $\mathbf{v}_i$ is the velocity and $\mathbf{F}_i$ is the force on particle i, $\mathbf{z}$ is a unit vector in the Z-direction, N is

the total number of particles in the system, and α is the Gaussian thermostatting multiplier given by

$$\alpha = \frac{\sum_{i=1}^{N} \mathbf{F}_i \left(\mathbf{p}_i - \mathbf{z} \frac{mQ_i J_z}{Q_i^2 N} \right)}{\sum_{i=1}^{N} \mathbf{p}_i \left(\mathbf{p}_i - \mathbf{z} \frac{mQ_i J_z}{Q_i^2 N} \right)}, \tag{2}$$

where

$$J_z = \sum_{i=1}^{N} Q_i v_{i,z} \tag{3}$$

is the electrical current induced in Z-direction by external field E_z. The temperature of the system follows from the constraint equation[1]

$$\frac{1}{m} \sum_{i=1}^{N} \left(\mathbf{p}_i - \mathbf{z} \frac{mQ_i J_z}{Q_i^2 N} \right)^2 = 3Nk_b T. \tag{4}$$

The calculation of steady state averages, such as the electrical current, by the NEMD method requires that a nonequilibrium steady state exists, i.e. that a thermal balance is maintained between the work done on the system by the applied electrical field and the heat removed by thermostat during the simulation run. Mathematically this relationship can be expressed as

$$3Nk_B T \langle \alpha \rangle = -\langle J_z(t) \rangle E_z, \tag{5}$$

where the left side represents the heat removed per unit time from the system by the thermostat and the right side is the energy dissipation rate for the system.

In applying this algorithm to conductivity phenomena, considering only the linear (or $E_z \to 0$) response to real oscillating or static fields, we start with the general relation[9]

$$\langle J_z(t) \rangle = \text{Re } \sigma^*(\omega) E_z(t) \tag{6}$$

where $\sigma^*(\omega)$ is by definition the Fourier transform of the equilibrium electrical current autocorrelation function

$$\sigma^*(\omega) = \frac{1}{k_B T} \int_0^\infty \langle J_z(0) J_z(t) \rangle_{\text{eq.}} e^{i\omega t} \, dt \tag{7}$$

and the field $E_z(t)$, is

$$E_z(t) = \text{Re } E_{z,0} e^{i\omega t}. \tag{8}$$

For real electrical fields the response of the ionic system is given by

$$\langle J_z(t) \rangle = \text{Re } J_{z,0} e^{i(\omega t + \varphi)}, \tag{9}$$

and the frequency dependent specific electrical conductivity, $\sigma(\omega)$, can be defined by the relation

$$\sigma(\omega) = \frac{1}{V} \text{Re } \sigma^*(\omega) = \lim_{E_{z,0} \to 0} \frac{J_{z,0}}{VE_{z,0}} \cos \varphi, \tag{10}$$

where V is the volume of the simulation cell. Hence, from the amplitude $J_{z,0}$ and the relative phase φ of the induced current one can calculate the electrical conductivity of the system at the frequency of interest[1]. For static electrical fields ($\omega = 0$) the specific conductivity is simply

$$\sigma_0 = \frac{1}{Vk_B T} \int_0^\infty \langle J_z(0) J_z(t) \rangle_{\text{eq.}} \, dt = \lim_{E_{z,0} \to 0} \frac{J_{z,0}}{VE_{z,0}}. \tag{11}$$

3. COMPUTATIONAL DETAILS AND POTENTIAL MODEL

In the present study we consider a fluid of charged soft spheres with the pair potential of the form

$$u(r) = u_{ss}(r) + u_Q(r), \tag{12a}$$

where

$$u_{ss}(r) = 4\varepsilon_{ss}\left(\frac{d}{r}\right)^{12} \tag{12b}$$

is the soft-sphere potential and

$$u_Q(r) = \frac{Q_1 Q_2}{r} \tag{12c}$$

is the Coulomb potential. The present model is characterized by the numerical parameters $\rho^* = \rho d^3 = 0.8$, $T^* = k_B T/\varepsilon_{ss} = 4.836$, $Q^* = (Q^2/\varepsilon_{ss} d)^{1/2} = \pm 13.272$, where

ρ^*, T^*, and Q^* are the reduced density, temperature and charge, respectively. In order to convert our transport coefficients from the reduced units used exclusively in our calculations into real units, we have chosen a particular set of molecular quantities ($4\varepsilon_{ss}/k_B = 1265°$ K, $d = 3$ Å, $m_{+-} = 23$ a.u.) employed in earlier work[10].

All NEMD simulations were carried out for systems of 108 (54 + 54) particles, while equilibrium runs were performed for both $N = 108$ (E1) and 256 (E2). In our calculations we have utilized periodic boundary conditions[10] and truncated octahedral geometry for the simulation cell[8]. The Ewald summation technique was used to evaluate the long range forces, with conducting boundary being applied. In our implementation the real space sum was carried over all nearest images, the Fourier space sum was truncated after the first 341 independent lattice vectors (corresponding to $n^2 \leq 49$) and the value of the convergence parameter, κ, was 6.75. For the short-range interactions we used a spherical cutoff at the $(\sqrt{3}/4)\,L$), where L is the length of the cube containing the truncated octahedron.

The equations of motion were integrated using a fourth order Gear algorithm[11] and a reduced time step $\Delta t/\tau = 0.0015$, where $\tau = \sqrt{md^2/\varepsilon_{ss}}$. In order to achieve sufficient precision in the current autocorrelation functions ($\sim 4\%$ for $N = 108$ and $\sim 3\%$ for $N = 256$), all our equilibrium MD simulations were run at least for 200000 timesteps. NEMD runs with applied static fields were usually 100000 timesteps in length giving a numerical uncertainty in the electrical conductivity of about 3%. NEMD simulations at high-frequency (in the dispersion region of the electrical conductivity) achieved the same precision with shorter runs (about 50000–80000 timesteps), although in a few cases longer NEMD calculations (about 200000 timesteps) were also performed. Eq. (5) was always satisfied to within statistical uncertainty in all our nonequilibrium runs.

4 RESULTS AND DISCUSSION

(*a*) *Thermodynamic and Structural Properties*

The average Coulombic energy, $\langle U_Q \rangle / N\varepsilon_{ss}$, and the average total configurational energy $\langle U \rangle / N\varepsilon_{ss}$, of the equilibrium molten salt (108 and 256 ions) are reported in Table 1. A separate MD simulation was carried out for the system of 108 particles

Table 1 Equilibrium results for a dense fluid at $\rho^* = 0.8$, $T^* = 4.836$ and $Q^* = 13.272$

N	$\dfrac{\langle U_Q \rangle}{N\varepsilon_{ss}}$	$\dfrac{\langle U \rangle}{N\varepsilon_{ss}}$	σ_0, *mho/cm*
108	-141.781 ± 0.010	-128.446 ± 0.009	2.20 ± 0.08
256	-141.626 ± 0.008	-128.208 ± 0.007	2.17 ± 0.05
108†	-141.361 ± 0.011	-128.551 ± 0.010	2.29 ± 0.09

† The results for a system in which the short-range potential between like-charged ions was omitted.

(hereafter referred to as E3) in which the short-range interactions between like-charged ions were omitted in order to allow direct comparison with earlier work[10]. The electrical conductivity for this system is also presented in Table 1. As we might expect, the thermodynamic properties are essentially independent of the number of particles and of the details of the short-range potential. The present calculation is in close agreement with previously published results[10].

The equilibrium structural properties of molten salts have been studied extensively in earlier MD simulations[9,10,12]. In the present investigation we have compared the equilibrium radial distribution functions (RDF) for systems of 108 and 256 ions as well as for E3 with results from previous equilibrium MD calculations[10] with $N = 216$ and potentials identical to those of E3. Again, the agreement with published results was very good. The form of soft-sphere potential and the system size were observed to have negligible effect.

Unlike equilibrium structural properties, the distribution of charges in a non-equilibrium electrolyte had previously not been examined. In this study we were able to detect the changes in ionic packing in a nonequilibrium ionic fluid in our constant field NEMD simulations for sufficiently large $E_{Z,0}$. In Figure 1 we have plotted the nonequilibrium distribution functions $g_{+-}(r, \theta = 0)$ and $g_{+-}(r, \theta = 180)$ for unlike ions in the largest examined electrical field $E^*_{z,0} = 2.0(1.5 \cdot 10^7$ V/cm). The equilibrium RDF has also been included in Figure 1 for comparison. The nonequilibrium distributions shown in Figure 1 are steady-state averages of the binary correlations within particular spatial sectors of interest, and equilibrium $g_{+-}(r)$ is the usual average all over the entire angular space. We define θ as the angle between the

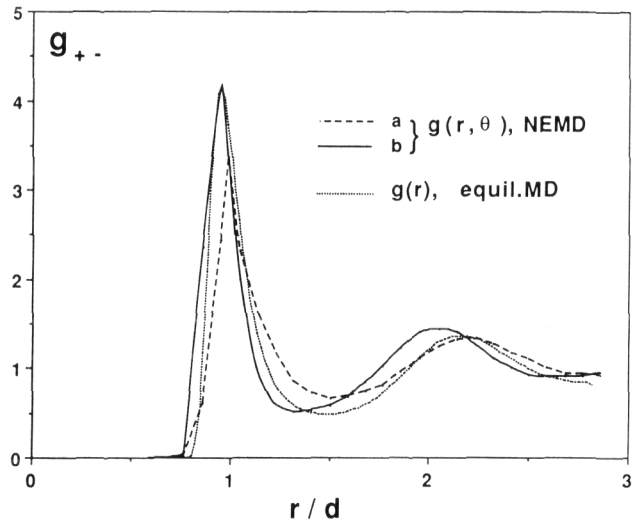

Figure 1 Comparison of equilibrium and nonequilibrium pair distribution functions for unlike-charged ions in a molten salt. For the nonequilibrium distributions (a) is $g_{+-}(r, \theta = 180)$, the charge distribution behind the ion moving in an external electric field, and (b) is $g_{+-}(r, \theta = 0)$ the distribution in front of the ion.

field-vector and the separation-vector. Hence the nonequilibrium distribution function $g_{+-}(r, \theta = 0)$ represents the distribution of unlike particles in front of an ion moving in a flow, whereas $g_{+-}(r, \theta = 180)$ reflects the distribution behind the ion.

As can be seen in Figure 1, this rather large applied electrical field perturbs the equilibrium structure of the fluid to the extent that spherical symmetry no longer exists in the interionic binary correlations. Our calculations indicate that both first and second ionic shells of the nonequilibrium structure are affected. Compression of the ionic shells is observed in front of moving ions; the first and particularly the second neighbor shells are shifted toward smaller interparticle separations. The first minimum of $g_{+-}(r, \theta = 0)$ is also shifted inward, but retains its depth. In the opposite direction ($\theta = 180$) the fluid becomes less structured; the first peak in $g_{+-}(r, \theta = 180)$ is significantly decreased and shifted to larger separations partially filling the first minimum, while similar, but less dramatic, changes are observed in the second maximum.

(*b*) *Transport properties*

The values of the static electrical conductivity, σ_0, have been calculated in our NEMD simulations with 108 particles using Eq. (11). Static fields ranging from 0.1 to 2.0 were employed and the results are shown in Figure 2. Values for σ_0 obtained from equilibrium MD simulation data (from the integral over the current autocorrelation function) for this molten salt are given in Table 1, with the 108 particle point included in Figure 2. Comparison of the present NEMD results with those of Evans and Morriss for Lennard-Jones fluids[1] indicates that the static electrical conductivity of this molten salt behaves in a manner very similar to that of the "color diffusion" constant of Lennard-Jones particles.

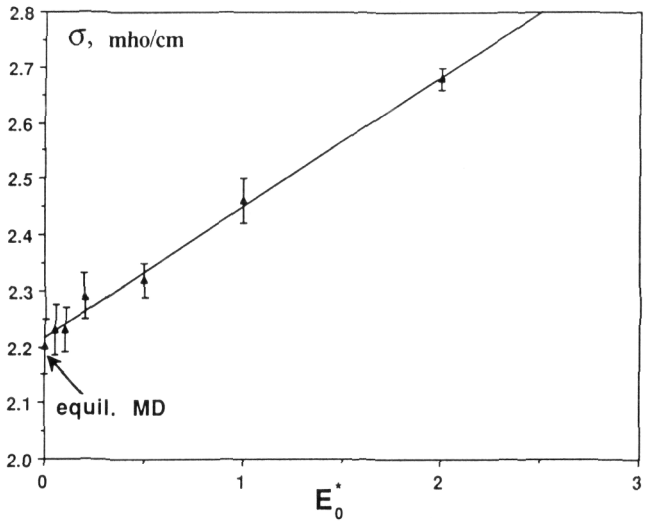

Figure 2 The dependence of specific conductivity of a molten salt on applied field strength obtained from static field NEMD simulations.

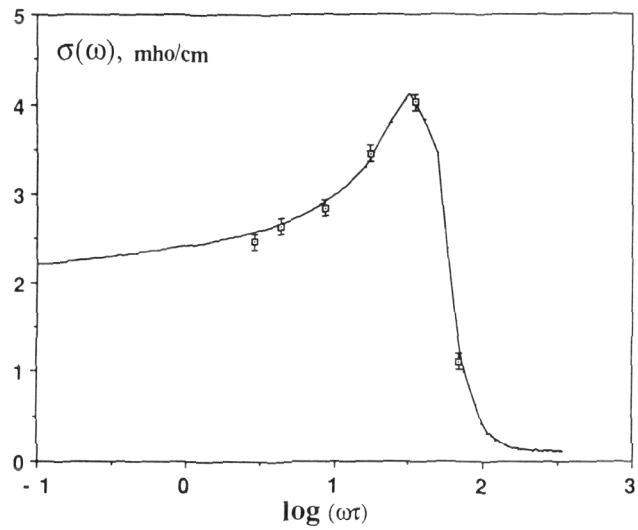

Figure 3 The spectrum of electrical conductivity of a molten salt. The solid line represents the Fourier transform of the equilibrium current autocorrelation function. The open squares are the results obtained from nonequilibrium simulations with alternating fields.

An important part of this work has been the investigation of the frequency dependent behavior of induced currents. It is clear from previous equilibrium simulations[10,12,13] and from the present study that the conductivity spectrum of molten salts possesses a well-defined maximum. The electrical conductivity spectrum for the present $N = 108$ system, calculated by the Fourier transform of the current autocorrelation function, is shown in Figure 3. This curve and the corresponding result for the 256 particle system are essentially identical.

In this study, NEMD techniques have been used to sample several individual frequencies on the spectrum and the results can also be found in Figure 3. The NEMD points agree within statistical uncertainty with the spectrum of current fluctuations at equilibrium. In Figure 4 we have shown the corresponding phase behavior of induced currents outside $\log \omega\tau = 1.24$ and within $\log \omega\tau = 1.84$ the dispersion region of the electrical conductivity. We observe that the current and applied field are essentially in phase at the frequency $\log \omega\tau = 1.24$ (Figure 4a), whereas at the frequency $\log \omega\tau = 1.84$ (Figure 4b) the phase lag is considerable, approaching its maximum value of $\pi/2$.

CONCLUSION

In this study we have used both equilibrium and nonequilibrium MD to examine the structural, thermodynamic and transport properties of a molten salt. Alternative methods for the evaluation of electrical conductivity were considered and the influence of applied electrical fields, both static and time-dependent, was explored.

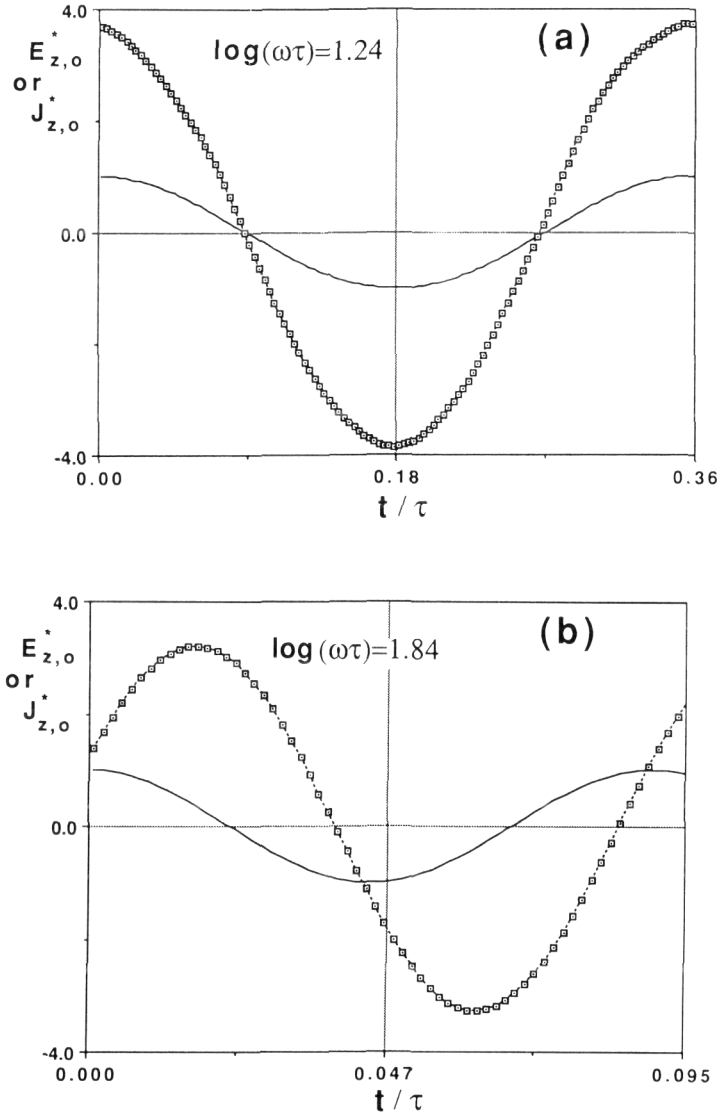

Figure 4 Phase behavior of induced alternating electrical currents. (a) Electrical response of a molten salt to a low-frequency electrical field. (b) Electrical response to a high-frequency electrical field. In both Figures the solid line is the applied field and the square represent the induced electrical currents.

The static electrical conductivity was determined in both our equilibrium and nonequilibrium MD simulations. The NEMD technique as applied to this ionic fluid was found to be at least as computationally efficient as the equilibrium calculation (considering the total time required and the statistical uncertainty in the conductivity values obtained).

In our calculations with static applied fields, a nonspherical packing structure around an ion in a molten salt was observed, illustrated by a directional dependence in the pair distribution function. Generally, the liquid behind the ion moving in an external electric field is less structured then at equilibrium, while a significant compression is observed in front of the ion. Further studies employing a similar approach may clarify further the molecular picture of charge transport in electrolyte solutions, plasmas and complex models[14,15].

NEMD techniques were used also to sample specific frequencies of the electrical conductivity spectrum of the molten salt. It proved to be an efficient tool, particularly when examining high-frequency oscillating fields. We remark that current investigations of coulombic gas[16] strongly suggest that NEMD becomes far more efficient in the low ionic density regime.

A ts

We are grateful for the financial support of the Natural Sciences and Engineering Research Council of Canada.

References

1. D. J. Evans and J. P. Morriss, Statistical Mechanics of Liquids, Academic, San Diego (1990).
2. W. G. Hoover, Computational Statistical Mechanics, Elsevier, New York (1991).
3. D. W. Heerman, Computer Simulations Methods in Theoretical Physics, Springer-Verlag, Berlin (1986).
4. (a) D. J. Evans and J. P. Morriss, *Phys. Rev. Lett.,* 51, 1776 (1983).
4. (b) D. J. Evans and J. P. Morriss, *Phys Rev.,* **A31,** 3817 (1985).
5. D. J. Evans and P. T. *Phys.,* **72,** 893 (1991).
6. D. J. Evans and J. P. Morriss, *Phys. Rev. Lett.,* 56, 2172 (1986).
7. D. MacGowan and D. J. Evans, *Phys. Rev.,* **A34,** 2133 (1986).
8. D. and D. M. Heyes, *Adv. Phys.,* 63, 493 (1985).
9. J. P. Hansen and I. R. McDonald, Theory of Simple Liquids, 2nd Edition, Academic, London (1986).
10. S. W. de Leeuw and J. W. *Physica,* 179 (1981).
11. D. J. Evans and J. P. Morriss, *Phys. Rep.,* 1, 297 (1984).
12. J. P. Hansen and I. R. McDonald, *Phys. Rev.,* **A11,** 2111 (1975).
13. G. Ciccotti, G. Jacucci and I. R. McDonald, *Phys. Rev.,* **A13,** 426 (1975).
14. J. M. Caillol, D. Levesque and J. J. Weis, *Chem. Phys.,* 85, 6645 (1986); **91,** 5555 (1989).
15. R. R. Dogonadze, E. A. A. and J. The Chemical Physics of Solvation, Elsevier, Amsterdam (1986).
16. I. M. Svishchev and P. G. Kusalik, *Physica,* **192A,** 628